NIH Public Access
Author Manuscript
Hypertension. Author manuscript; available in PMC 2009 June 9.

Published in final edited form as:
Hypertension. 2008 August ; 52(2): 279–286. doi:10.1161/HYPERTENSIONAHA.108.109819.

Marked Regional Left Ventricular Heterogeneity in Hypertensive Left Ventricular Hypertrophy Patients:

A Losartan Intervention for Endpoint Reduction in Hypertension (LIFE) Cardiovascular Magnetic Resonance and Echocardiographic Substudy

Robert W.W. Biederman, **Mark Doyle**, **Alistair A. Young**, **Richard B. Devereux**, **Eduardo Kortright**, **Gilbert Perry**, **Jonathan N. Bella**, **Suzanne Oparil**, **David Calhoun**, **Gerald M. Pohost**, and **Louis J. Dell'Italia**
Division of Cardiology, Department of Cardiovascular MRI, Gerald McGuiness Center, Allegheny General Hospital (R.W.W.B., M.D.), Pittsburgh, Pa; University of Auckland (A.A.Y.), New Zealand; Division of Cardiology (R.B.D.), Weill Cornell Medical College, New York, NY; ACTEK, Inc (E.K.), Birmingham, Ala; University of Alabama at Birmingham (G.P., S.O., D.C., L.J.D.); Bronx-Lebanon Hospital Center (J.N.B.), Bronx, NY; and the Division of Cardiology (G.M.P.), University of Southern California, Los Angeles.

Abstract

Concentric hypertensive left ventricular (LV) hypertrophy is presumed to be a symmetrical process. Using MRI-derived intramyocardial strain, we sought to determine whether segmental deformation was also symmetrical, as suggested by echocardiography. High echocardiographic LV relative wall thickness in hypertensive LV hypertrophy allows preserved endocardial excursion despite depressed LV midwall shortening (MWS). Depressed MWS is an adverse prognostic indicator, but whether this is related to global or regional myocardial depression is unknown. We prospectively compared MWS derived from linear echocardiographic dimensions with MR strain(∈) in septal and posterior locations in 27 subjects with ECG LV hypertrophy in the Losartan Intervention for Endpoint Reduction in Hypertension Study. Although MRI-derived mass was higher in patients than in normal control subjects (124.0±38.6 versus 60.5±13.2g/m^2; P<0.001), fractional shortening (30±5% versus 33±3%) and end-systolic stress (175±22 versus 146±28 g/cm^2) did not differ between groups. However, mean MR(∈) was decreased in patients versus normal control subjects (13.9±6.8% versus 22.4±3.5%), as was echo MWS (13.4±2.8% versus 18.2±1.4%; both P<0.001). For patients versus normal control subjects, posterior wall(∈) was not different (17.8±7.1% versus 21.6±4.0%), whereas septal(∈) was markedly depressed (10.1±6.6% versus 23.2±3.4%; P<0.001). Although global MWS by echocardiography or MRI is depressed in hypertensive LV hypertrophy, MRI tissue tagging demonstrates substantial regional intramyocardial strain(∈) heterogeneity, with most severely depressed strain patterns in the septum. Although posterior wall 2D principal strain was inversely

© 2008 American Heart Association, Inc.

Correspondence to Robert W.W. Biederman, Allegheny General Hospital, 320 E North Ave, Pittsburgh, PA 15212. E-mail E-mail: rbiederm@wpahs.com.

Disclosures

R.B.D. has received research grants and honoraria from Merck & Co, Inc (Merck), and fees as a consultant and member of the speaker's bureaux of Merck and Novartis. S.O. has received research grants from Daiichi-Sankyo, Novartis, and Sanofi Aventis; grants-in-aid from Abbott Laboratories, Astra Zeneca, Aventis, Biovail, Boehringer-Ingelheim, Bristol Myers-Squibb, Forest Laboratories, Glaxo-SmithKline, Novartis, Merck, Pfizer, Sankyo Pharma, Sanofi-Synthelabo, and Schering-Plough; fees as a member of the speaker's bureaux for Boehringer-Ingelheim, Bristol Myers-Squibb, Daiichi, Merck, Novartis, Pfizer, the Salt Institute, Sankyo, and Sanofi Aventis; fees as a consultant/advisory board member for Bristol Myers-Squibb, Daiichi Sankyo, Merck, Novartis, Pfizer, the Salt Institute, and Sanofi Aventis; and fees as a member of the board of directors for Encysive Pharmaceuticals. The remaining authors report no conflicts.

NIH-PA Author Manuscript
NIH-PA Author Manuscript
NIH-PA Author Manuscript

NIH-PA Author Manuscript

NIH-PA Author Manuscript

NIH-PA Author Manuscript

related to radius of curvature, septal strain was not, suggesting that factors other than afterload are responsible for pronounced myocardial strain heterogeneity in concentric hypertrophy.

Keywords

heart function; hypertension; hypertrophy; heart failure; radius of curvature; strain patterns

Left ventricular hypertrophy (LVH) is a major adaptive response to chronic pressure overload and a powerful independent predictor of adverse cardiovascular events in hypertension.[1-3] However, indicators of left ventricular (LV) endocardial shortening, such as fractional shortening and ejection fraction (EF), do not predict cardiovascular events. LV midwall shortening (MWS), an indirect measure of myocardial performance assessed by transthoracic echocardiography, is decreased in a subset of patients with hypertensive LVH.[4-7] Patients with LVH and decreased MWS are at increased risk for cardiovascular events despite normal endocardial fractional shortening.[2] Functional studies of isolated papillary muscles from experimental models of chronic pressure overload demonstrated depressed contractility despite normal EF.[8-10] Taken together, these findings suggest that depressed MWS identifies a maladaptive hypertrophic response in the continuum of adaptation to chronic pressure overload and serves as an important clinical predictor in patients with hypertensive LVH.

Echocardiographic calculation of MWS is a geometry-based index derived from linear measurements of the posterior and the septal walls and, consequently, cannot distinguish between septal versus posterior wall function. Thus, whether depressed MWS represents global or regional intrinsic depression of LV myocardial function in pressure-overload hypertrophy is unknown. Previous experiments demonstrated that increased LV pressure could have dissimilar effects on regional LV wall stress because of different radii of curvature, resulting in regional mechanical heterogeneity because of dissimilar afterload.[11,12] MRI tissue tagging allows intramyocardial displacement and strain to be measured noninvasively by monitoring motion of identifiable material points distributed throughout the myocardium.[13-16] We hypothesized that wide sampling of the myocardium using a nongeometric method, MRI tissue tagging, would identify regional heterogeneity of LV myocardial function in patients with hypertensive LVH. To our knowledge, there has been no direct comparison of echocardiographic MWS and MRI tissue tagging in patients with documented hypertensive LVH.

We evaluated patients enrolled in the Losartan Intervention For Endpoint reduction in hypertension (LIFE) Study and normal subjects to test the hypothesis that regional assessment of LV myocardial function by MRI tissue tagging would correspond globally with echocardiographic MWS but would also reveal segmental intramyocardial dysfunction in patients with significant LVH but preserved chamber function.

Methods

Patients

Patients 55 to 80 years old with arterial pressures 160 to 200/95 to 115 mm Hg were eligible if their ECG demonstrated LVH by Cornell voltage-duration product ($R_{aVL}+S_{V3}$ [+6 mm in women]×QRS duration >2440 mm · ms) or Sokolow-Lyon voltage ($SV_1+RV_5–V_6$>38 mm) criteria.[17,18] Patients with known LV EF <40% or myocardial infarction within 6 months were excluded. Nineteen (7 women) of 25 patients (76%), aged 56 to 78 years, with no history or clinical evidence of heart failure entered the MRI substudy. All of the patients had normal LV EF (>60%) except for 1 patient who had percutaneous transluminal coronary angioplasty twice in the past 5 years (EF: 51%). After 2 weeks of washout of antihypertensive therapies,

NIH-PA Author Manuscript

NIH-PA Author Manuscript

NIH-PA Author Manuscript

patients underwent transthoracic echocardiography and MRI tissue tagging within 24 hours. Eight normotensive volunteers (7 men) aged 25 to 38 years without history of cardiac disease underwent identical examinations. The protocol was approved by the institutional review board at the University of Alabama at Birmingham. All of the subjects gave written informed consent.

Echocardiography

Blood pressures were recorded by mercury sphygmomanometer before and after echocardiography. 2D targeted M-mode and 2D echocardiograms were recorded using a 2.25-MHz probe and a commercially available phased-array Hewlett Packard instrument. Linear septal and posterior wall thicknesses (PWTs) and LV chamber dimensions were measured from M-mode or 2D recordings according to American Society of Echocardiography methods.[19-22]

Derived Echocardiographic Parameters

Echocardiographic MWS was calculated according to previously described methods of de Simone et al.[2,5,23,24] LV end-systolic circumferential stress (σc) was calculated according to methods described by Aurigemma et al.[4] Relative wall thickness, the index of the geometric pattern of hypertrophy, was calculated as 2 times the PWT/LV end-diastolic dimension; relative wall thickness >0.44 is consistent with concentric LV geometry.[25]

Magnetic Resonance Imaging

MRI was performed with a 1.5T scanner (ACS Philips). Scan parameters were repetition time/echo time/flip, 50/7.6/30 ms; slice thickness, 8 mm; field of view, 300 mm; matrix, 256×256; and frame duration, 30 to 40 ms. After orthogonal scout scans, the 2- and 4-chamber long-axis views were acquired by triggered ECG R wave. Orthogonal tags were applied using common k-space techniques.[26] A single short-axis tag was produced by a 6-element binomial pulse with a composite flip angle of 160°, producing a tag spacing of 6 mm. Nontagged images from the 2 long-axis views were used to define short-axis planes. Six to 10 short-axis nontagged sections were acquired, covering base to apex with an intersection gap of 4 to 6 mm.

Tagged images were acquired using modified respiratory ordered phase encoding compensation strategies taking input from abdominal belt and bellows (Figures 1 and 2).[27] K-space lines were synchronized with the respiratory cycle in a similar fashion to respiratory ordered phase encoding except that respiratory segments with highest excursion data were not acquired.

Investigators blinded to echocardiographic data performed all of the quantitative strain analyses. An MRI short-axis view was selected at the mitral valve leaflet tips, approximating echocardio-graphic acquisitions. The 2D strain analysis was performed using SPAMMVU.[28,29] Tag intersection points created myocardial triangular tiling.[14] End-systolic to end-diastolic deformation within triangles was measured, and eigenvalues and eigenvectors of the Lagrangian strain tensors were calculated. Maximum strain in each region formed the principal strain.

Strain data were related to each individual's heart by resolving the principal strain into local circumferential and radial components. All of the strains were expressed as a percentage as follows:

$$\varepsilon = \frac{\ell - \ell_0}{\ell} \times 100\%$$

NIH-PA Author Manuscript

NIH-PA Author Manuscript

NIH-PA Author Manuscript

where ℓ is the underformed length (end diastole) and ℓ_0 is the deformed length (end systole). Circumferential strain is negative indicating myocardial shortening, whereas radial strain is positive, indicating thickening of primarily circumferentially oriented LV fibers.

To compare echo MWS directly with MRI strains, strains were analyzed in the anterior septum and posterior walls at the level of the mitral leaflet tips. These regions correspond with those used for parasternal LV linear echocardiographic measurements in the LIFE Study (Figure 3A and 3B). LV mass by MRI was calculated from short-axis data using standard techniques.[30]

To examine relations between regional strains and radius of curvature, curvature was measured in the long- and short-axis planes. Curvature was defined as 1/r, where "r" is the radius of a circular arc. Curvature analysis was performed in a Matlab environment fitting an arc at the midwall of each region of interest by manually placing arc handles with a mouse evaluated at sections of interest.

Statistical Analysis

All of the data are presented as means±SDs. Means were compared using Student *t* tests (unpaired or paired). Two-tailed $P<0.05$ was considered statistically significant.

Heterogeneity of circumferential strain for the entire short axis was assessed by ANOVA after data passed normality and equal variance tests. Significance ($P<0.05$) was accepted for all of the pairwise multiple comparisons with Bonferroni correction (between regions). The Kruskal-Wallis ANOVA was performed on nonnormally distributed data. Regional differences between groups were assessed by 2-way ANOVA with posthoc Tukey test.

Power calculations for circumferential and radial strains to detect >0.06% change (normal variance) for patients versus control subjects yielded the following powers at $\alpha=0.05$: circumferential septal strain (power=0.99), radial septal strain (power=0.96), circumferential posterior wall strain (power=0.40), and radial posterior wall strain (power=0.15).

Results

Population Characteristics

Fractional shortening, end-systolic circumferential wall stress, LV end-diastolic dimension, and LV end-systolic dimension did not differ significantly between patient and control groups (Table 1). As expected, patients had higher mean end-diastolic posterior and septal wall thicknesses and relative wall thickness than control subjects. Importantly, among patients there was no difference between mean septal and PWTs, consistent with symmetrical concentric hypertrophy. LV mass by MRI was >2-fold greater in LVH versus control subjects and >3 SDs above normal. As has been described previously, MRI mass was less than echocardio-graphic LV mass.[31,32]

Strain Analysis

In patients versus control subjects, mean MRI circumferential strain (24 to 28 loci evaluations per patient) was depressed, as was echocardiographic MWS (Table 2). Although mean echocardiographic MWS and MRI circumferential strain were similar in patients (13.4% versus 13.9%, respectively), there was only modest correlation between the 2 measurements ($r=0.46$; $P<0.05$). Moreover, comparisons between wall segments composing the M-mode measurements of MWS revealed marked heterogeneity. In the posterior wall (Figure 4), MRI circumferential and radial strains were not significantly depressed in patients versus normal control subjects. However, MRI circumferential and radial strains in the septum were markedly and significantly decreased in patients (by 56% and 42%, respectively; Figure 5; $P<0.001$ and

NIH-PA Author Manuscript

NIH-PA Author Manuscript

NIH-PA Author Manuscript

$P<0.05$, respectively, versus the posterior wall). However, in normal control subjects, septal and posterior wall circumferential and radial strains were similar. Thus, in patients with LVH, despite similar septal and PWTs, normal end-systolic circumferential stress, and preserved chamber shortening, septal strain was markedly depressed, whereas posterior wall strain was relatively unaffected by the hyper-trophic process.

However, it is unlikely that the 2 regions used to estimate MWS by echocardiography depict all of the regional heterogeneity in intramyocardial strain present in the section. Therefore, we divided the entire LV short-axis section into 18 equal regions of 20° increments around the circumference. Figure 6A plots mean circumferential strain for these regions for patients and normal control subjects (14.6±6.3% versus 18.2±7%; $P=<0.00004$). Patients' circumferential shortening was most depressed in the septum and inferior wall, whereas anterior wall strain approached that of normal control subjects, and inferolateral wall strain was intermediate between septal and anterior wall strain values. Thus, function of hypertrophied LV walls differs by location within the heart such that myocardial regions farthest from the septum possess the greatest strain. Figure 6B diagrammatically displays the corresponding LV short-axis reference regions for Figure 6A. When the LV was further divided into 6 regions of 60° corresponding to commonly accepted clinical territories, circumferential strains were markedly lower in all of the regions except the inferolateral wall ($P=0.000011$). Compared with normal control subjects, all of the regions in patients had markedly reduced circumferential strains except the anterior and anterolateral walls, which were virtually identical ($P<0.05$).

Curvature Analysis

Mean curvatures (1/r) were uniformly, albeit not significantly, lower in the septum versus posterior wall for patients and normal control subjects (Table 3). Combining the short-and long-axis curvatures revealed a negative relationship with 2D principal intramyocardial strain in the normal and LVH groups for the posterior wall ($r=-0.86$, $P=0.033$ and $r=-0.55$, $P=0.017$, respectively) but not for the septum ($r=0.23$, $P=0.55$ and $r=0.56$, $P=0.39$, respectively).

Discussion

In patients with LVH, low MWS despite preserved LV chamber function constitutes a negative prognostic indicator.[2] However, it was heretofore unknown whether this index reflected global or regional depression of LV myocardial function. The current investigation demonstrates that MWS by echocardiography and mean circumferential strain by MRI tissue tagging were significantly and similarly depressed in patients with hypertensive LVH but preserved LV chamber function. However, regional assessment of LV strain by MRI tagging demonstrated that hypertensive LVH patients experienced segmental reduction function, most pronounced in the interventricular septum with a >60% lower circumferential strain than normal control subjects, whereas posterior wall strain showed no significant difference between patients and normal control subjects. This suggests that depressed circumferential shortening seen by echocardiographic MWS reflects near-normal posterior wall function combined with severely depressed septal mechanics; ie, depressed MWS in hypertensive LVH with preserved LV chamber function does not predict a symmetrical contraction pattern. Furthermore, for the posterior wall in patients and normal control subjects, there was a significant relationship between wall curvature and principal strain, accounting for the observed circumferential strain. However, no such relationship was found for the septum, suggesting that abnormal afterload is not the driving force for its depressed strain. This supports observations of earlier investigators,[33-35] who suggested that forces (and resultant mechanics) acting on the interventricular septum, but not the free wall, are multifactorial.

In the patient group, curvatures of the septal and posterior walls were decreased relative to normal control subjects indicating that geometric remodeling, not just wall thickening, plays

NIH-PA Author Manuscript

NIH-PA Author Manuscript

NIH-PA Author Manuscript

a role in the hypertrophic process. This curvature was correlated with principal strain in the posterior wall in patients and normal control subjects, suggesting the posterior wall conforms more classically to Laplacian models of circumferential stress. Lack of correlation between curvature and septal strain suggests that other factors fashion the resultant septal function, likely RV interaction, fiber orientation, rigidity, wall thickness, and intrinsic myocardial function.

Heretofore it was unknown whether decreased MWS in patients with hypertensive LVH represented myocardial dys-function or was related to geometric assumptions inherent in calculations of MWS. Examining the calculation of MWS, any distance traveled by the midwall will be inherently reduced by a higher initial diastolic wall thickness. Indeed, LV MWS correlates inversely with LV mass and relative wall thickness.[2] According to the mathematical formula of de Simone et al[5] used here, MWS necessarily decreases as LV geometry becomes more concentric. Furthermore, echocardiographic calculation of MWS is designed to represent a global index derived from posterior and septal walls; consequently, it cannot distinguish between septal versus posterior wall performance.

The current investigation demonstrates agreement of means with only modest correlation between echocardio-graphic MWS and mean MRI circumferential strain. However, by regional strain analysis (Figure 6), the septum is preferentially depressed, whereas the posterior wall is relatively normal. Although we were primarily interested in the 2 regions subtended by the echocardiographic examination, an analysis of circumferential variation of circumferential strain showed that the observed intramyocardial depressed strain was not unique to the septum. Indeed, circumferential strain was heterogeneous, being relatively unaffected in the anterior wall, whereas inferolateral wall strain was intermediate between that of the anterior and septal walls but greater than inferior wall strain.

For the first time we have demonstrated that, despite uniform and symmetrical (concentric) LVH, regional myocardial contraction is far from uniform or symmetrical. Although other investigators have raised the possibility of such a finding, methodologic limitations have prevented unambiguous interpretation. Masuyama et al,[36] using integrated backscatter in pressure overload models, demonstrated isolated septal dysfunction in aortic stenosis patients with LVH. Their septal/posterior wall ratio was 1.24:1.00 (14.7:11.9 mm), suggesting that the predominate pathology was disproportionately upper septal thickening. In contrast, our septal/posterior wall ratios were nearly identical (1.04 and 1.06 in LVH and controls, respectively). van Rugge et al[37] noted regional wall motion differences between the septum and posterior walls after MRI dobutamine stress in normal control subjects, but that study did not include patients with LVH.

To our knowledge, only 1 other study evaluated hypertensive LVH patients using MRI tissue tagging. Palmon et al[16] demonstrated depressed circumferential and longitudinal strain patterns with only mild echocardiographic LVH, normal ECGs, and normal EFs. However, they did not find the magnitude of disproportionate septal dysfunction that we identified. Notable population differences were the presence of ECG-defined LVH and substantially greater echocardio-graphic LV mass in our group (163±52 versus 127±37 g/m^2). Furthermore, our patients had antihypertensive medication withheld for 2 weeks, whereas 21 of 30 patients in the study by Palmon et al[16] were on calcium channel blockers or β-blockers at imaging, potentially confounding intrinsic contractile investigations because of negative inotropy.

Our finding of disproportionate septal dysfunction in the setting of chronic pressure overload is an intriguing finding that may be related to the unique architecture and geometry of the septum. The finding of reduced segmental deformation in the setting of preserved chamber function may at first appear counterintuitive. However, when geometric considerations are

NIH-PA Author Manuscript

NIH-PA Author Manuscript

NIH-PA Author Manuscript

accounted for, the paradox is resolved. With progressive increases in wall thickness, progressive decreases in individual myocyte shortening are required to achieve similar (or greater) thickening and endocardial excursion. This is in keeping with the pathophysiology of hypertensive LVH that supports a compensatory hypertrophic process to normalize developed Laplacian stress.[7]

Limitations

A potential limitation of the current study is that we did not study age-matched controls. Normal data were acquired to validate the tagging protocol, yet our normal strains were in accord with others.[14,16] In addition, in an echocardiographic study of 464 clinically normal adults, Slotwiner et al[38] demonstrated that LV MWS did not differ in subjects across ages of 16 to 41, 41 to 54, and 54 to 88 years. Similar findings were observed by Palmon et al.[16] This argues against nonuniformity of myocardial contraction being an age-related phenomenon. Finally, our investigation was designed solely to explore the 2D nature of MWS by echocardiography related to MRI intramyocardial mechanics. A 3D strain analysis, beyond the scope of this investigation, could examine the local and global effects of the hypertensive LVH in greater detail.

Conclusions

To our knowledge, this study is the first to compare findings from echocardiographic MWS and MRI tissue tagging in hypertensive LVH patients. Although global MWS by echocardiography and average MRI circumferential strain are similarly depressed in hypertensive LVH, MRI demonstrates severely depressed strain localized to the septum in the face of preserved chamber function, normal end-systolic stress, and similar wall thicknesses. Symmetrical concentric LVH does not predict symmetrical LV contraction. The observed abnormal strain patterns may represent a novel marker for early regional myocardial dysfunction in LVH patients with otherwise preserved chamber function.

Perspectives

With the advent of cardiovascular MRI, the high spatial resolution affords a clinically relevant ability to evaluate myocardial characteristics often invisible by more traditional imaging modalities. Evidence from this study shows that it is no longer safe to assume that the apparent symmetrical contraction of concentric LVH is truly symmetrical until viewed with a high-fidelity imaging method such as MRI. Underlying anatopathologic considerations appear to exist that may account for this observation and may point toward further myocardial perturbations in LVH patients unrecognized previously by lower-resolution imaging. A 3D strain analysis may shed further insight into these observations in addition to confirming the 2D findings.

Acknowledgments

We greatly appreciate discussions with Nathaniel Reichek, MD, editorial assistance of Paulette A. Lyle, and statistical assistance of Diane Vido, MS.

Sources of Funding

This study was supported by the Office of Research and Development, Medical Service, Department of Veteran Affairs (to L.J.D.); National Heart, Lung, and Blood Institute grants RO1 HL54816 (to L.J.D.) and NHLBI TG HL07711 (to G.M.P.); American Heart Association National Scientist Development grant (R.W.W.B.); and a grant from Merck & Co, Inc. (R.W.W.B.). R.B.D., G.P., S.O., and D.C. were investigators and/or members of the LIFE Steering Committee and have received grant support from Merck & Co, Inc, the sponsor of the LIFE Study.

NIH-PA Author Manuscript

NIH-PA Author Manuscript

NIH-PA Author Manuscript

References

1. Koren MJ, Devereux RB, Casale PN, Savage DD, Laragh JH. Relation of left ventricular mass and geometry to morbidity and mortality in uncomplicated essential hypertension. Ann Int Med 1991;114:345–352. [PubMed: 1825164]
2. de Simone G, Devereux RB, Koren MJ, Mensah GA, Casale PN, Laragh JH. Midwall left ventricular mechanics. An independent predictor of cardiovascular risk in arterial hypertension. Circulation 1996;93:259–265. [PubMed: 8548897]
3. Levy D, Garrison RJ, Savage DD, Kannel WB, Castelli WP. Prognostic implications of echocardiographically determined left ventricular mass in the Framingham Heart Study. N Engl J Med 1990;322:1561–1566. [PubMed: 2139921]
4. Aurigemma GP, Silver KH, Priest MA, Gaasch WH. Geometric changes allow normal ejection fraction despite depressed myocardial shortening in left ventricular hypertrophy. J Am Coll Cardiol 1995;26:195–202. [PubMed: 7797752]
5. de Simone G, Devereux RB, Roman MJ, Ganau A, Saba PS, Alderman MH, Laragh JH. Assessment of left ventricular function by the midwall fractional shortening/end-systolic stress relation in human hypertension. J Am Coll Cardiol 1994;23:1444–1451. [PubMed: 8176105]
6. Shimizu G, Zile MR, Blaustein AS, Gaasch WH. Left ventricular chamber filling and midwall fiber lengthening in patients with left ventricular hypertrophy: overestimation of fiber velocities by conventional midwall measurements. Circulation 1985;71:266–272. [PubMed: 3155498]
7. Shimizu G, Hirota Y, Kita Y, Kawamura K, Saito T, Gaasch WH. Left ventricular midwall mechanics in systemic arterial hypertension. Myocardial function is depressed in pressure-overload hypertrophy. Circulation 1991;83:1676–1684. [PubMed: 1827056]
8. Bing OH, Matsushita S, Fanburg BL, Levine HJ. Mechanical properties of rat cardiac muscle during experimental hypertrophy. Circ Res 1971;28:234–245. [PubMed: 4251783]
9. Jacob R, Vogt M, Rupp H. Pathophysiologic mechanisms in cardiac insufficiency induced by chronic pressure overload–an attempt to analyze specific factors in animal experiment. Basic Res Cardiol 1986;81(suppl 1):203–216. [PubMed: 3790041]
10. Spann JF Jr, Buccino RA, Sonnenblick EH, Braunwald E. Contractile state of cardiac muscle obtained from cats with experimentally produced ventricular hypertrophy and heart failure. Circ Res 1967;21:341–354. [PubMed: 6061641]
11. Heng MK, Janz RF, Jobin J. Estimation of regional stress in the left ventricular septum and free wall: an echocardiographic study suggesting a mechanism for asymmetric septal hypertrophy. Am Heart J 1985;110:84–90. [PubMed: 3160227]
12. Lew WY, LeWinter MM. Regional comparison of midwall segment and area shortening in the canine left ventricle. Circ Res 1986;58:678–691. [PubMed: 3708765]
13. Axel L, Dougherty L. MR imaging of motion with spatial modulation of magnetization. Radiology 1989;171:841–845. [PubMed: 2717762]
14. Young AA, Imai H, Chang CN, Axel L. Two-dimensional left ventricular deformation during systole using magnetic resonance imaging with spatial modulation of magnetization. Circulation 1994;89:740–752. [PubMed: 8313563]
15. Clark NR, Reichek N, Bergey P, Hoffman EA, Brownson D, Palmon L, Axel L. Circumferential myocardial shortening in the normal human left ventricle. Assessment by magnetic resonance imaging using spatial modulation of magnetization. Circulation 1991;84:67–74. [PubMed: 2060124]
16. Palmon LC, Reichek N, Yeon SB, Clark NR, Brownson D, Hoffman E, Axel L. Intramural myocardial shortening in hypertensive left ventricular hypertrophy with normal pump function. Circulation 1994;89:122–131. [PubMed: 8281637]
17. Dahlöf B, Devereux R, de Faire U, Fyhrquist F, Hedner T, Ibsen H, Julius S, Kjeldsen S, Kristianson K, Lederballe-Pedersen O, Lindholm LH, Nieminen MS, Omvik P, Oparil S, Wedel H. The Losartan Intervention for Endpoint Reduction (LIFE) in Hypertension study: rationale, design, and methods. The LIFE Study Group. Am J Hypertens 1997;10:705–713. [PubMed: 9234823]
18. Dahlöf B, Devereux RB, Julius S, Kjeldsen SE, Beevers G, de Faire U, Fyhrquist F, Hedner T, Ibsen H, Kristianson K, Lederballe-Pedersen O, Lindholm LH, Nieminen MS, Omvik P, Oparil S, Wedel H. Characteristics of 9194 patients with left ventricular hypertrophy: the LIFE Study. Losartan

NIH-PA Author Manuscript

NIH-PA Author Manuscript

NIH-PA Author Manuscript

Intervention for Endpoint Reduction in Hypertension. Hypertension 1998;32:989–997. [PubMed: 9856962]

19. Sahn DJ, DeMaria A, Kisslo J, Weyman A. Recommendations regarding quantitation in M-mode echocardiography: results of a survey of echo-cardiographic measurements. Circulation 1978;58:1072–1083. [PubMed: 709763]
20. Schiller NB, Shah PM, Crawford M, DeMaria A, Devereux R, Feigenbaum H, Gutgesell H, Reichek N, Sahn D, Schnittger I, Silverman NH, Tajik J. Recommendations for quantitation of the left ventricle by two-dimensional echocardiography. American Society of Echocardiography Committee on Standards, Subcommittee on Quantitation of Two-Dimensional Echocardiograms. J Am Soc Echocardiogr 1989;2:358–367. [PubMed: 2698218]
21. Devereux RB, Alonso DR, Lutas EM, Gottlieb GJ, Campo E, Sachs I, Reichek N. Echocardiographic assessment of left ventricular hypertrophy: comparison to necropsy findings. Am J Cardiol 1986;57:450–458. [PubMed: 2936235]
22. Yurenev AP, DeQuattro V, Devereux RB. Hypertensive heart disease: relationship of silent ischemia to coronary artery disease of left ventricular hypertrophy. Am Heart J 1990;120:928–933. [PubMed: 2145735]
23. de Simone G, Daniels SR, Devereux RB, Meyer RA, Roman MJ, de Divitiis O, Alderman MH. Left ventricular mass and body size in normotensive children and adults: assessment of allometric relations and impact of overweight. J Am Coll Cardiol 1992;20:1251–1260. [PubMed: 1401629]
24. de Simone G, Devereux RB, Daniels SR, Koren MJ, Meyer RA, Laragh JH. Effect of growth on variability of left ventricular mass: assessment of allometric signals in adults and children and their capacity to predict cardiovascular risk. J Am Coll Cardiol 1995;25:1056–1062. [PubMed: 7897116]
25. Ganau A, Devereux RB, Roman MJ, de Simone G, Pickering TG, Saba PS, Vargiu P, Simongini I, Laragh JH. Patterns of left ventricular hypertrophy and geometric remodeling in essential hypertension. J Am Coll Cardiol 1992;19:1550–1558. [PubMed: 1534335]
26. Doyle M, Walsh EG, Foster RE, Pohost GM. Common k-space acquisition: a method to improve myocardial grid-tag contrast. Magn Reson Med 1997;37:754–763. [PubMed: 9126950]
27. Bailes DR, Gilderdale DJ, Bydder GM, Collins AG, Firmin DN. Respiratory ordered phase encoding (ROPE): a method for reducing respiratory motion artefacts in MR imaging. J Comput Assist Tomogr 1985;9:835–838. [PubMed: 4019854]
28. Axel L, Goncalves RC, Bloomgarden D. Regional heart motion: two-dimensional analysis and functional imaging with MR imaging. Radiology 1992;183:745–750. [PubMed: 1584931]
29. Young AA, Axel L, Dougherty L, Bogen DK, Parenteau CS. Validation of tagging with MR imaging to estimate material deformation. Radiology 1993;188:101–108. [PubMed: 8511281]
30. van der Geest RJ, Jansen E, Buller VGM, Reiber JHC. Automated detection of left ventricular epi- and endocardial contours in short-axis MR images. Comput Cardiol 1994:33–36.
31. Chuang ML, Beaudin RA, Riley MF, Mooney MG, Mannin WJ, Douglas PS, Hibberd MG. Three-dimensional echocardiographic measurement of left ventricular mass: comparison with magnetic resonance imaging and two-dimensional echocardiographic determinations in man. Int J Card Imaging 2000;16:347–357. [PubMed: 11215919]
32. Stewart GA, Foster J, Cowan M, Rooney E, McDonagh T, Dargie HJ, Rodger RS, Jardine AG. Echocardiography overestimates left ventricular mass in hemodialysis patients relative to MRI. Kidney Int 1999;56:2248–2253. [PubMed: 10594802]
33. Armour JA, Lippincott DB, Randall WC. Functional anatomy of the interventricular septum. Cardiology 1973;58:65–79. [PubMed: 4750797]
34. Streeter DD Jr, Spotnitz HM, Patel DP, Ross J Jr, Sonnenblick EH. Fiber orientation in canine left ventricle during diastole and systole. Circ Res 1969;24:339–347. [PubMed: 5766515]
35. Janz RF, Ozpetek S, Ginzton LE, Laks MM. Regional stress in a non-circular cylinder. Biophys J 1989;55:173–182. [PubMed: 2930818]
36. Masuyama T, St Goar FG, Tye TL, Oppenheim G, Schnittger I, Popp RL. Ultrasonic tissue characterization of human hypertrophied hearts in vivo with cardiac cycle-dependent variation in integrated backscatter. Circulation 1989;80:925–934. [PubMed: 2529060]

NIH-PA Author Manuscript

NIH-PA Author Manuscript

NIH-PA Author Manuscript

37. van Rugge FP, Holman ER, van der Wall EE, de Roos A, van der Laarse A, Bruschke AV. Quantitation of global and regional left ventricular function by cine magnetic resonance imaging during dobutamine stress in normal human subjects. Eur Heart J 1993;14:456–463. [PubMed: 8472707]

38. Slotwiner DJ, Devereux RB, Schwartz JE, Pickering TG, de Simone G, Ganau A, Saba PS, Roman MJ. Relation of age to left ventricular function in clinically normal adults. Am J Cardiol 1998;82:621–626. [PubMed: 9732891]

NIH-PA Author Manuscript
NIH-PA Author Manuscript
NIH-PA Author Manuscript

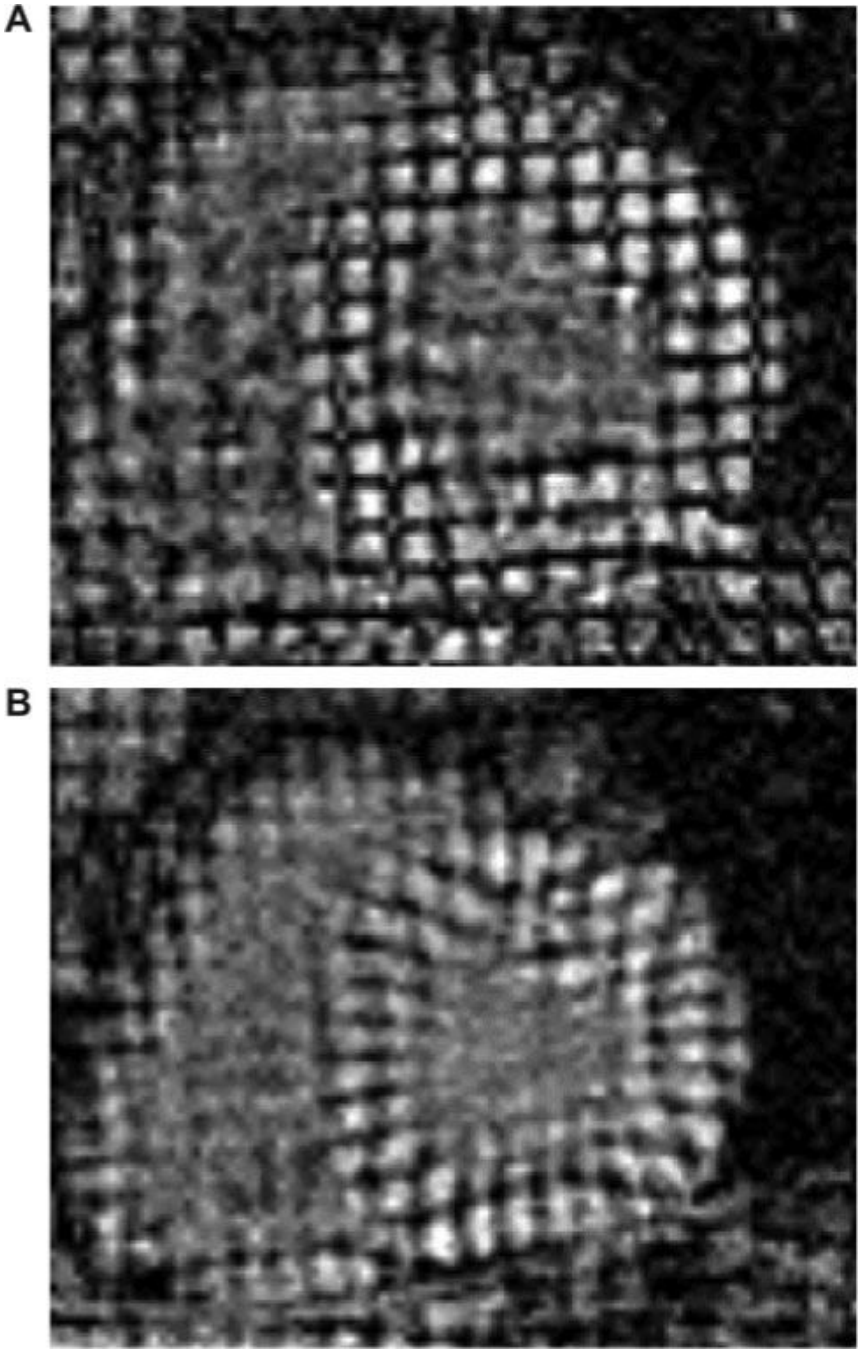

Figure 1.
MRI short-axis tissue tags in a normal subject illustrating normal wall thickness and high-resolution tagging. Vertices of tagging stripes at end diastole (A) and end systole (B) were tracked yielding circumferential and radial strain. Visual inspection alone reveals normal septal deformation.

NIH-PA Author Manuscript

NIH-PA Author Manuscript

NIH-PA Author Manuscript

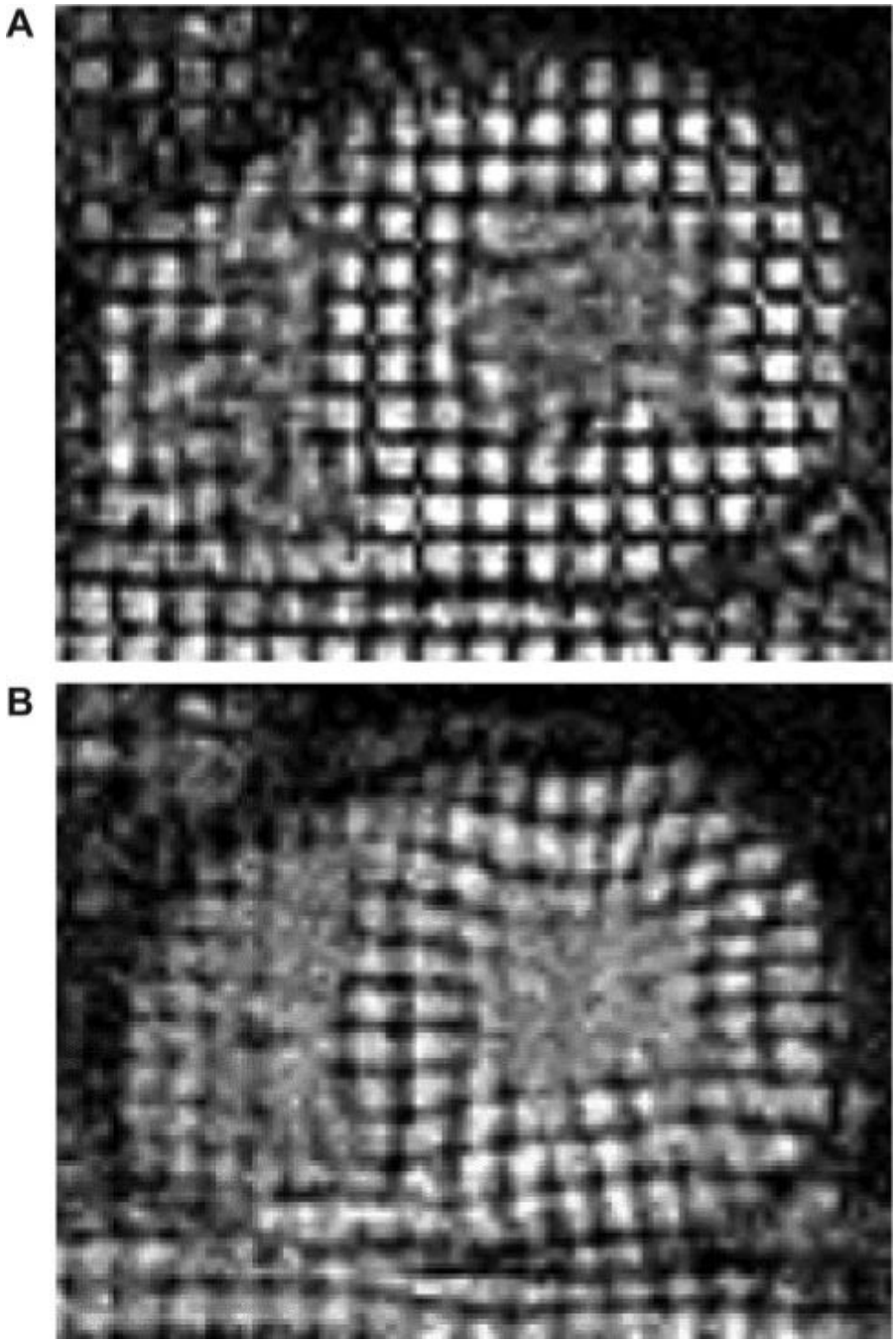

Figure 2.
MRI tissue-tagged images in a patient with hypertensive LVH with increased wall thickness. Visual inspection reveals diminished septal deformation between end diastole (A) and end systole (B).

NIH-PA Author Manuscript
NIH-PA Author Manuscript
NIH-PA Author Manuscript

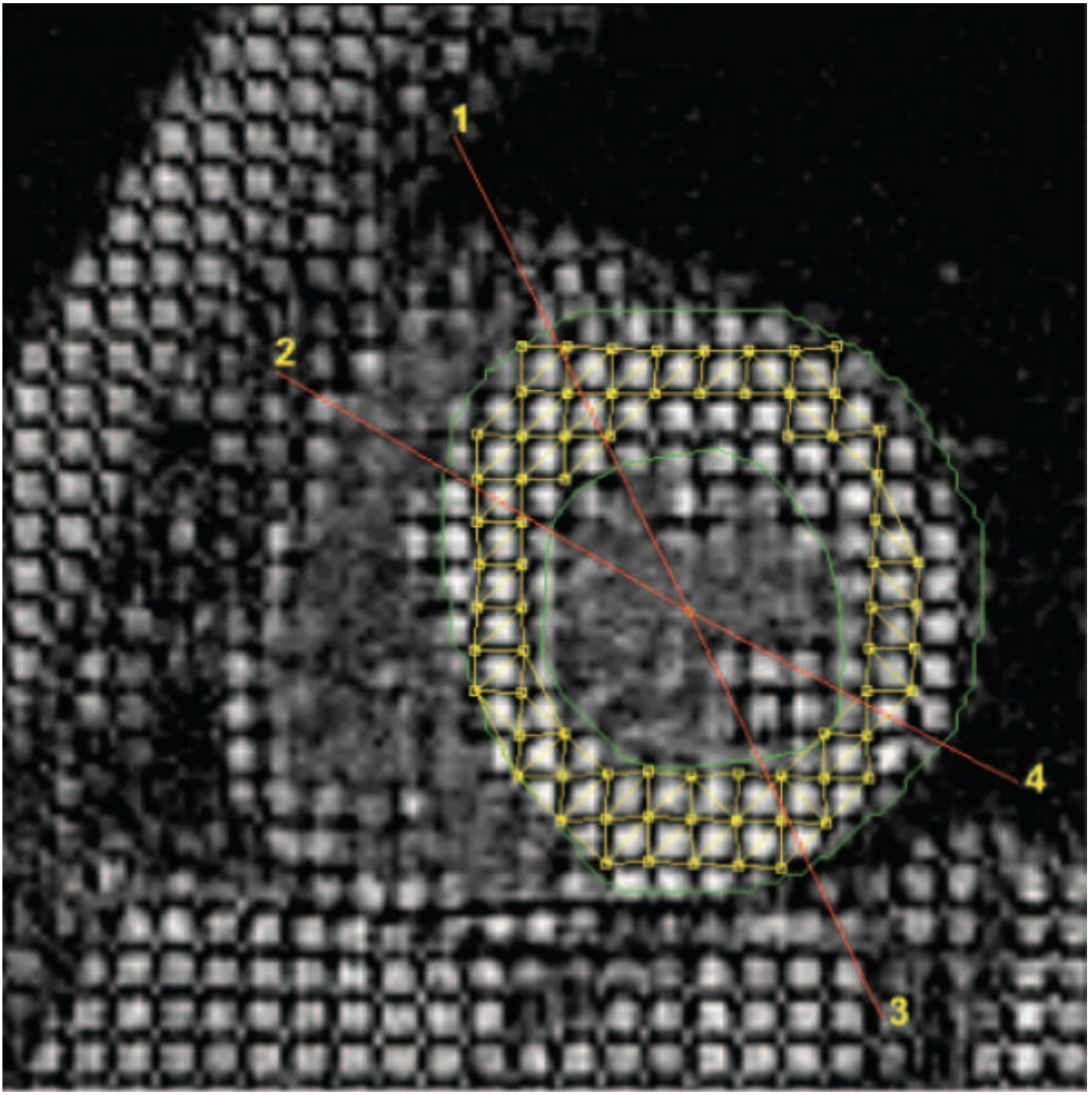

Figure 3.
Short-axis view depicting MRI interrogations similar to echocardiography in the parasternal-long axis. The anterior septum is between regions 1 and 2. The posterior wall is between 3 and 4. Note the midwall triangulation tiling deformation pattern used to determine strain between end diastole and end systole.

NIH-PA Author Manuscript

NIH-PA Author Manuscript

NIH-PA Author Manuscript

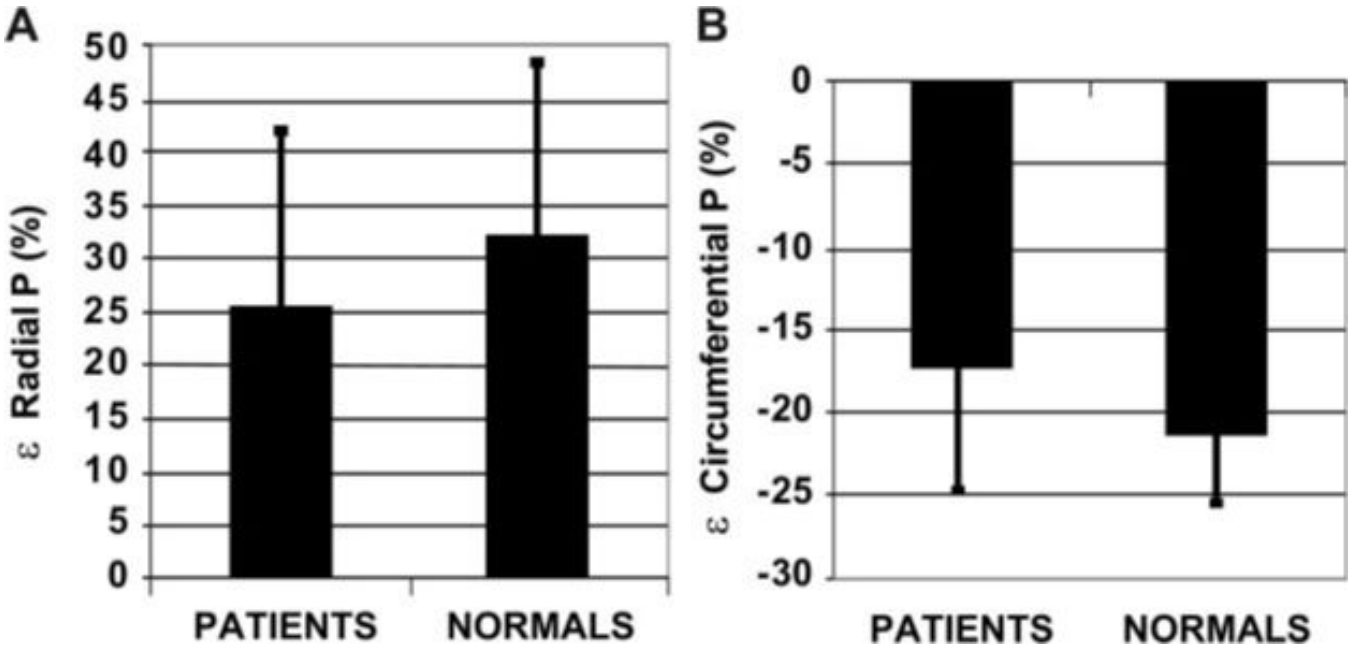

Figure 4.

Bar graphs of radial (A) and circumferential (B) posterior wall strain∈ expressed as the percentage of deformation (%) in patients vs normal control subjects (*P* value not signifi-cant for both).

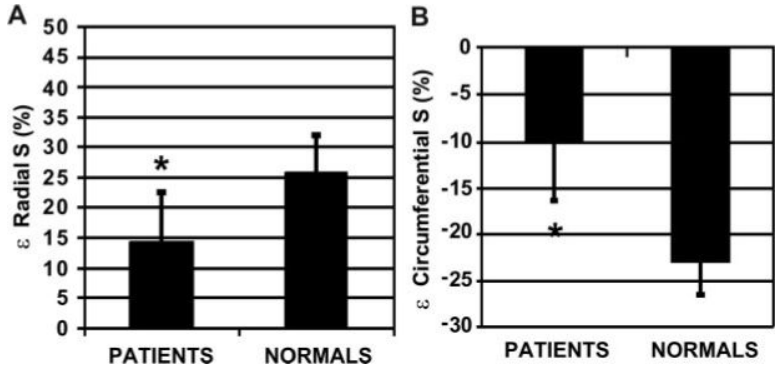

Figure 5.
Bar graphs of radial (A) and circumferential (B) septal strain∈ expressed as the percentage of deformation (%) in patients vs normal control subjects (*P<0.001).

NIH-PA Author Manuscript
NIH-PA Author Manuscript
NIH-PA Author Manuscript

NIH-PA Author Manuscript

NIH-PA Author Manuscript

NIH-PA Author Manuscript

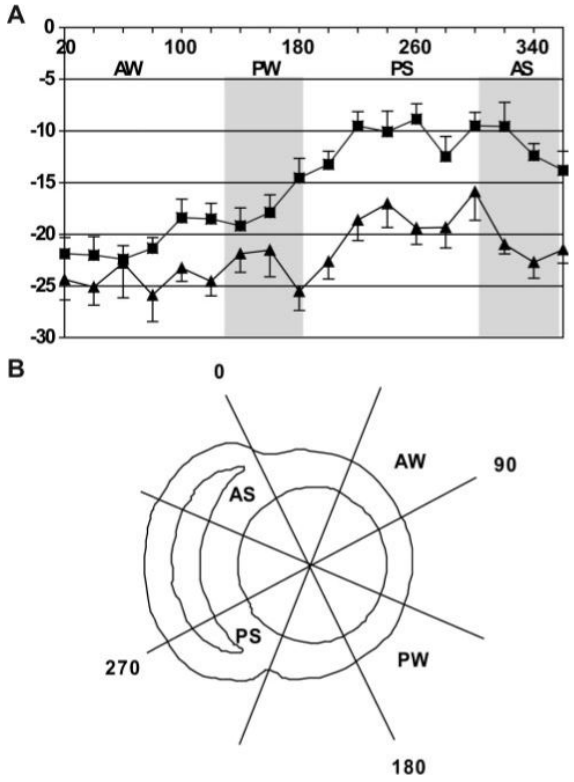

Figure 6.

Circumferential strain is displayed every 20° around the LV short axis. Zero degrees corresponds with interventricular septal-anterior wall junction, progressing in a clockwise direction (observed from the apex) through 360°. Squares indicate patients; triangles, control subjects. Data are means±SEs. The anterior septum (AS; 315° to 360°) and inferolateral walls (PW; 135° to 180°) are highlighted in gray. In LVH, anteroseptal circumferential strain is markedly depressed vs the inferolateral wall, whereas the 2 regions are indistinguishable in normal control subjects. Fitting a sine function curve to the radial distribution of circumferential strain (fit comprises amplitude, mean level, and phase) revealed that the 2 curves are significantly different in their means ($P<0.0001$), further supporting markedly altered circumferential strain patterns in LVH despite preserved LV function. B, Short-axis schematic for the regions of interest.

NIH-PA Author Manuscript

NIH-PA Author Manuscript

NIH-PA Author Manuscript

Table 1

Population Characteristics

Characteristic	Patients	Normal Controls
Sex	14 M, 5 F	7 M, 1 F
Blood pressure, mm Hg	178/94±14/14*	119/70±9/5*
Posterior wall thickness diastole, cm	1.24±0.22*	0.75±0.08*
Septal wall thickness diastole, cm	1.29±0.24*	0.79±0.06*
Septal/posterior wall ratio	1.00:1.04	1.00:1.05
LV end-diastolic dimension, cm	5.21±0.36	5.00±0.44
LV end-systolic dimension, cm	3.63±0.35	3.34±0.37
End-diastolic posterior wall thickness, cm	1.24±0.21†	0.75±0.08†
End-diastolic septal wall thickness, cm	1.29±0.24†	0.79±0.06†
Relative wall thickness	0.48±0.08*	0.30±0.03*
LV mass by MRI, g	220.4±73.7†	121.0±24.2†
LV mass/BSA by MRI, g/m^2	97.5±32.6†	55.7±11.2g†
LV mass by echocardiography, $g/m^{2.7}$	65.7±23.4†	28.1±6.0†
LV mass by echocardiography, g	280±87†	131±29†
LV mass/BSA by echocardiography, g/m^2	163±52†	74±15†

BSA indicates body surface area; F, females; M, males.

*Patients vs normal control subjects: $P<0.001$.

†Patients vs normal control subjects: $P<0.0001$.

NIH-PA Author Manuscript

NIH-PA Author Manuscript

NIH-PA Author Manuscript

Table 2

Cardiac Function Characteristics

Characteristic	Patients	Normal Controls
End-systolic circumferential stress, g/cm^2	175±22	146±28
Fractional shortening, %	30±5	33±3
EF, %	58.7±8.3	61.7±5.9
Echocardiographic MWS, %	13.4±2.8*	18.2±1.4*
Mean MRI circumferential strain (in analogous MWS segment)	13.9±6.8*	22.4±3.5*
Posterior wall circumferential strain, %	−17.8±7.1	−21.6±4.0
Posterior wall radial strain, %	23.6±16.5	32.2±16.3
Septal wall circumferential strain, %	−10.1±6.6*	−23.2±3.4*
Septal wall radial strain, %	14.9±8.1*	25.9±6.1*

*Patients vs normal control subjects: $P<0.001$.

NIH-PA Author Manuscript

NIH-PA Author Manuscript

NIH-PA Author Manuscript

Table 3

Radii of Curvature

Group	Posterior Wall	Septal Wall	Posterior Wall	Septal Wall
LVH	34±8	31±8	13±4	8±3
Normal controls	37±8	33±3	14±3	6±4

Data are 1/r, 10×10^{-2} cm (*P* value was not significant for all).